Discover Chemical Engineering

Discover

Research

Solubility of $Na_2O{\cdot}xAl_2O_3$ in NaF-KF-AlF_3-based low-temperature electrolyte

Ye Kuang[1] · Hengwei Yan[1,2] · Zhanwei Liu[1,2] · Yonghui Yang[1]

Received: 6 February 2023 / Accepted: 21 April 2023
Published online: 27 April 2023

Abstract
The solubility of $Na_2O{\cdot}xAl_2O_3$ in a NaF-KF-AlF_3-based low-temperature electrolyte was investigated, and the influence of electrolyte temperature at 750 ℃, *CR* = 1.3–1.4, CaF_2, and LiF on the alumina solubility was studied. The dissolution rate of alumina in the electrolyte was determined by measuring the alumina concentration in the electrolyte at different times with an oxygen analyzer. The results showed that in the NaF-KF-AlF_3-based low-temperature electrolyte, the dissolution rate of alumina in $Na_2O{\cdot}xAl_2O_3$ was faster than that of Al_2O_3. As the Na_2O content in alumina increased, the dissolution rate increased. Similarly, a higher *CR* of NaF-KF-AlF_3 and a higher temperature of the molten salt (750–850 °C) increased the dissolution rate of alumina in the electrolyte. The dissolution rate of alumina in NaF-KF-AlF_3 decreased after adding CaF_2 and LiF. According to the kinetics analysis, the dissolution rate of alumina followed the zero-order reaction rate law from 0–5 min, which showed that it depended on the amount of alumina absorbed in the electrolyte in the first five minutes.

Keywords Low-temperature aluminum electrolysis · NaF-KF-AlF_3-based · Alumina concentration · The dissolution rate of alumina

1 Introduction

Hall-Héroult cryolite-alumina molten salt electrolysis is the primary method for producing aluminum, but it uses carbon anodes that are directly consumed, which generates about 1.5 tons of CO_2 per ton of aluminum. Furthermore, this process emits about 0.75 (t CO_2e/t Al) of perfluorocarbons (PFCs), and the primary aluminum industry is faced with increasingly strict global restrictions on greenhouse gas emissions [1]. The Hall-Héroult method has become very mature after more than 130 years of continuous improvements, and there is very limited room for technological progress.

Carbon-free aluminum electrolysis based on inert anodes uses low-consumption inert electrodes instead of carbon anodes. This process emits oxygen during electrolysis and produces no greenhouse gases or hazardous gases such as CO_2, SO_2, or PFCs. Low-temperature aluminum electrolysis can extend the service life of inert electrodes; thus, inert electrode aluminum electrolysis is more likely to be successful only when combined with low-temperature aluminum electrolysis to achieve zero carbon emissions during aluminum electrolysis [2, 3].

Supplementary Information The online version contains supplementary material available at https://doi.org/10.1007/s43938-023-00027-4.

✉ Hengwei Yan, 476178577@qq.com | [1]Faculty of Metallurgical and Energy Engineering, Kunming University of Science and Technology, Kunming 650093, China. [2]National Engineering Laboratory for Vacuum Metallurgy, Kunming University of Science and Technology, Kunming 650093, China.

Since Sleepy et al [4] first proposed the concept of low-temperature aluminum electrolysis in 1979, researchers have carried out many subsequent studies on it [5–8]. However, the lower the temperature, the slower the dissolution rate of alumina, especially below 750 ℃. The biggest problem of low-temperature aluminum electrolysis is that the dissolution rate of alumina in the electrolyte is too slow to keep pace with the electrolytic consumption rate of alumina. This can lead to catastrophic corrosion of the anode and contamination of primary aluminum using non-carbon inert anodes [9].

Beck [10] proposed the concept of suspended alumina electrolysis to increase the alumina dissolution rate during low-temperature aluminum electrolysis. The method involved placing the anode at the bottom of the electrolytic cell. During electrolysis, the gases produced by the anode suspend alumina particles, but this increases the costs and reduces the current efficiency.

Although the KF-AlF_3 system has a lower liquidus temperature and better alumina solubility, it inevitably transforms into a NaF-KF-AlF_3 system as electrolysis proceeds, and sodium in the alumina feedstock accumulates in the electrolyte [11–13]. A preliminary study [8] showed that the introduction of a small amount of NaF (0–5 mol%) into the KF-AlF_3 electrolyte with a cryolite ratio ($CR = M_{KF}/M_{AlF3}$) of 1.2–1.7 sharply increased the initial crystallization temperature. This easily caused the electrolyte to crust at the cathode during electrolysis, making the KF-AlF_3 electrolyte unsuitable for industrial applications. The NaF-KF-AlF_3 system is a low-temperature electrolyte system that has attracted attention only in recent years. The NaF-KF-AlF_3 electrolyte with a low cryolite ratio ($CR = (M_{NaF} + M_{KF})/M_{AlF3}$) has a lower initial crystallization temperature, which solves the problems caused by the accumulation of NaF during electrolysis of the KF-AlF_3 electrolyte system. This system is the most promising low-temperature aluminum electrolyte system for industrial applications [14–16]. However, at temperatures below 800 ℃ and high contents of CaF_2 and LiF in the electrolyte, the solubility of alumina in NaF-KF-AlF_3 at mole ratios in the range of 1.3–1.4 and NaF content of 30 mol% is low, and its dissolution rate is slow [16, 17].

In this paper, a small amount of Na_2O was added to Al_2O_3 to produce β-Al_2O_3 by calcination to promote the dissolution rate of alumina in the electrolyte. $Na_2O{\cdot}xAl_2O_3$ (x is the MR of Al_2O_3 to Na_2O) samples with different molar ratio (MR) values were formulated, pressed, and calcined. Then, the solubility of the calcined pressed disc samples in NaF-KF-AlF_3 low-temperature electrolyte was measured. The $Na_2O{\cdot}xAl_2O_3$ raw material with the lowest possible Na_2O addition amount and fast Al_2O_3 dissolution rate was obtained.

2 Experimental

2.1 Chemical and experimental setup

The experimental materials included potassium fluoride (KF), sodium fluoride (NaF), aluminum hydroxide ($Al(OH)_3$), polyvinyl alcohol ($[\text{-}CH_2CHOH\text{-}]_n$), sodium hydroxide (NaOH), and aluminum fluoride (AlF_3). All reagents were placed into a vacuum chamber and dried at 120 ℃ for 24 h and stored in an airtight container until use. A LECO oxygen analyzer (RO500, LECO Corporation, St. Joseph, MI, USA) was used to determine the oxygen content in $Na_2O{\cdot}xAl_2O_3$ in the electrolyte. The alumina content of the sample was determined by the oxygen content.

1—stainless steel sampling rod; 2—corundum tube (argon inlet); 3—copper pipe (cooling water inlet); 4—O-ring; 5—corundum furnace tube; 6—heat insulation sheet group; 7—graphite crucible; 8—molten salt; 9-$Na_2O{\cdot}xAl_2O_3$ tablets; 10—stainless steel positioning rod; 11—brass ring; 12—fastening bolts; 13—brass cover.

As shown in Fig. 1, the experimental setup and procedure for determining the alumina concentration in the electrolyte were similar to those used by Yan et al. [15, 16]. Dried NaF, KF, and AlF_3 were weighed according to the cryolite ratio (CR). The mixed materials were quickly transferred into a high-purity graphite crucible. The calcined $Na_2O{\cdot}xAl_2O_3$ pressed disc was fixed on a tungsten wire.

To reduce the volatilization of molten salt during the experiment, a graphite lid was attached to the graphite crucible. A $Na_2O{\cdot}xAl_2O_3$ disc was hung above the melt before starting the furnace. The furnace was started, and then the air-cooled industrial chiller was turned on, and high-purity argon gas was introduced. After heating to the required temperature, the furnace was held for 1 h to ensure that all of the electrolyte was melted. Then, the $Na_2O{\cdot}xAl_2O_3$ disc was placed into the melt, and a stainless steel rod was used to take samples at intervals through the hole in the graphite lid.

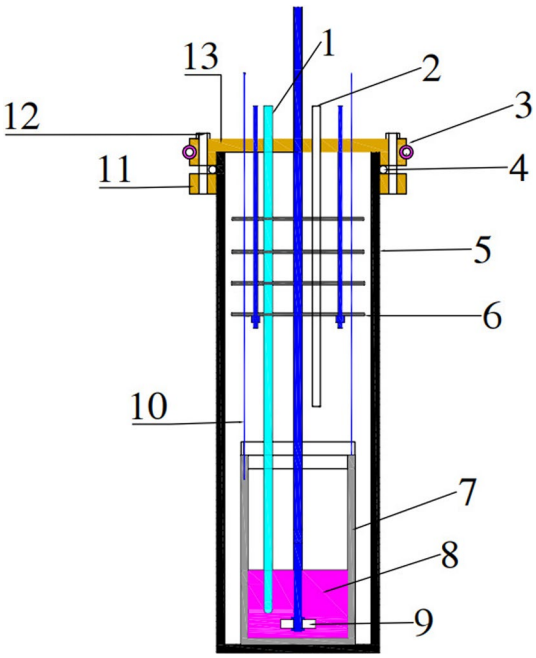

Fig. 1 Schematic diagram of the device for measuring aluminum solubility

2.2 Experimental process

The experimental protocol was performed by using Na_2O and Al_2O_3 in MR of 1: 50, 1: 70, and 1: 90. The blank Al_2O_3 samples were formed from $Al(OH)_3$. The sodium dioxide content of the investigated ratios is shown in Table 1.

Metallurgical-grade alumina was produced by the Bayer process. Due to the use of sodium hydroxide solution as the solvent, the Na_2O content in the alumina products is generally 0.2–0.4 wt%. During alumina production by the Bayer process, alumina with a higher Na_2O content can be obtained by controlling the washing degree of aluminum hydroxide. [18]

The proportioned reagent was mixed with 5 wt% of total reagent mass deionized water and 5 wt% polyvinyl alcohol. This mixture was heated until boiling and then placed into a vacuum-drying oven at 100 ℃ for 12 h. After that, it was pressed into flakes, which were loaded into a corundum crucible for calcination at 1000 ℃.

The electrolyte was mixed and put into the graphite crucible, two calcined $Na_2O{\cdot}xAl_2O_3$ flakes were perforated, and the tungsten wire and fixed with clips above the interior of the graphite crucible. The high-temperature well resistance furnace was controlled to heat up from room temperature to different temperatures at a heating rate of 3 ℃·min^{-1}. When the temperature reached the value, the furnace was held for 1 h. After the temperature was constant, immersed the sample in the electrolyte to start the test, and samples were at 3 min, 5 min, 10 min, 60 min, 120 min, and 240 min. When collecting the solidified electrolyte, the crusted material on the stainless steel rod was scraped off. The cooled solid electrolyte sample was put into a sample bag for drying and storage. After drying, the sample was measured by a LECO oxygen meter to determine the oxygen content in the electrolyte, which was then converted to alumina concentration. The formulas for calculating the Al_2O_3 content of $Na_2O{\cdot}xAl_2O_3$ in the melt are:

$$W_{Al_2O_3} = 2.125 \cdot O_{Al_2O_3} \tag{1}$$

$$o_{Al_2O_3} = O_{LECO} - O_{Na_2o} \tag{2}$$

Table 1 Effect of $Na_2O{\cdot}xAl_2O_3$ as raw material on electrolytic aluminum

	x (MR) value in $Na_2O{\cdot}xAl_2O_3$		
	50	70	90
Na_2O content/wt%	1.20	0.86	0.67

$$o_{LECO} = a + x \cdot a \cdot b \cdot \frac{16}{62} \tag{3}$$

$$o_{Na_2o} = X \cdot b \cdot a \cdot \frac{16}{62} \quad \left(b = \frac{16}{X \cdot 164}\right) \tag{4}$$

where O_{LECO} is the result detected by the oxygen analyzer, x is the MR of Al_2O_3 to Na_2O, b refers to the percentage of Na_2O in $Na_2O{\cdot}70Al_2O_3$, and a refers to the percentage of O in Al_2O_3.

The dissolution rate over a specific time period was calculated as follows. The dissolution rate of $Na_2O{\cdot}xAl_2O_3$ in the electrolyte under each condition was calculated in segments by calculating the dissolution rate of alumina at each time period. For example, the dissolution rate of alumina in the time period T_2–T_1 is given by (5):

$$\overline{V} = \frac{S_2 - S_1}{T_2 - T_1} \tag{5}$$

where S_1 and S_2 are the alumina content in the electrolyte at T_1 and T_2, respectively.

3 Results and discussion

3.1 Study of the structure of $Na_2O{\cdot}xAl_2O_3$ at different MR

The samples of $Na_2O{\cdot}xAl_2O_3$ (x = 0, 50, 70, 90) were calcined at 1000 ℃ and then characterized by XRD. Powder diffraction data were obtained using a PANalytical X'pert PRO diffractometer with CuKα radiation. The detector was equipped with a graphite monochromator. All the XRD patterns were baseline adjusted and smoothed.

As shown in Fig. 2, phases in $Na_2O{\cdot}x(50, 70, 90)$ Al_2O_3 calcined at 1000 ℃ included β-Al_2O_3 and α-Al_2O_3, and $Na_2O{\cdot}x(50, 70)$ Al_2O_3 contained a small amount of γ-Al_2O_3. In Fig. 2, the intensity of the β-Al_2O_3 diffraction peak in $Na_2O{\cdot}50Al_2O_3$ was the highest, while $Na_2O{\cdot}90Al_2O_3$ was the smallest. As shown in supplementary Fig. S-1, because of the formation of β-Al_2O_3 when Na_2O in $Na_2O{\cdot}xAl_2O_3$ solidified, the β-Al_2O_3 system formed a Na/O layered structure that the other phases of alumina did not have. The different structure led to the faster dissolution rate of β-Al_2O_3 in the electrolyte [19].

3.2 Effect of different MR on the solubility of $Na_2O{\cdot}xAl_2O_3$ in NaF-KF-AlF_3

$Na_2O{\cdot}xAl_2O_3$ was put into the electrolyte, and the concentration of alumina in NaF-KF-AlF_3 with a CR = 1.6 and a NaF content of 30 mol% was determined at 850 °C. The results are shown in Fig. 3.

In NaF-KF-AlF_3, the alumina concentration of $Na_2O{\cdot}xAl_2O_3$ increased gradually upon increasing the dissolution time. From 0 to 10 min, the concentration of alumina changed the most, indicating that the dissolution rate of $Na_2O{\cdot}xAl_2O_3$ in the electrolyte was the fastest during this period. From 0 to 60 min, it was found that the concentration of the blank

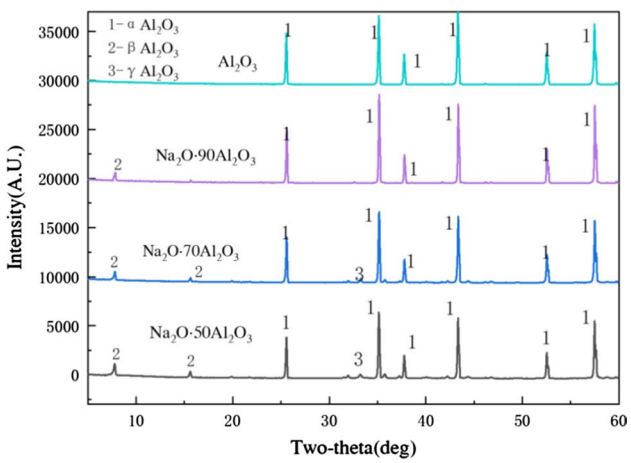

Fig. 2 Effect of MR on the structure of $Na_2O{\cdot}xAl_2O_3$ after calcination at 1000 ℃

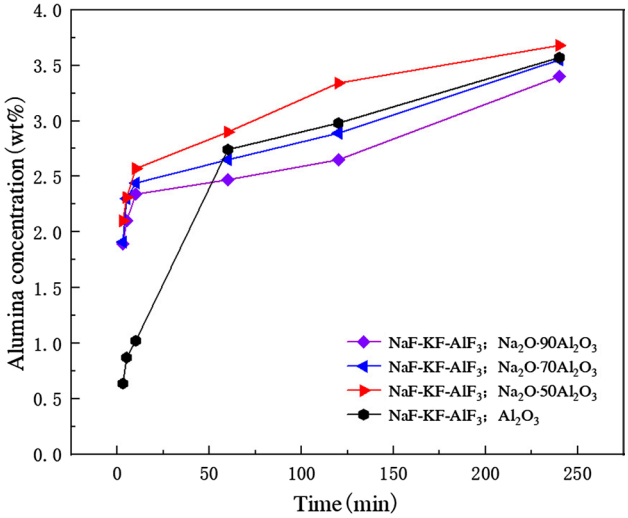

Fig. 3 Effect of different MR on the dissolution properties of $Na_2O{\cdot}xAl_2O_3$ in NaF-KF-AlF_3

Al_2O_3 sample in the electrolyte was lower than that of $Na_2O{\cdot}xAl_2O_3$. The difference between the two concentrations was about 1.43 wt%, which was about 2.6 times. When dissolved for 240 min, the concentration of $Na_2O{\cdot}$(50, 70, 90) Al_2O_3 and blank Al_2O_3 sample decreases gradually. The lower the MR, the higher the Na_2O content, and the faster the dissolution rate.

The dissolution rate of alumina in the electrolyte was calculated based on the change between each time sampled, as shown in Fig. 4.

Upon increasing the reaction time, the dissolution rate of alumina in the electrolyte gradually decreased. At 0–5 min, the dissolution rate of $Na_2O{\cdot}50Al_2O_3$ in the electrolyte was faster than the dissolution rate of alumina in samples with other MR values. In the first 5 min, the dissolution rate of the blank Al_2O_3 sample was the slowest. The dissolution rate of $Na_2O{\cdot}$(50, 70, 90)Al_2O_3 in the electrolyte was 3.2–2.7 times higher than that of the blank Al_2O_3 sample.

3.3 Effect of CR on the solubility of $Na_2O{\cdot}70Al_2O_3$ in electrolytes

In the NaF-KF-AlF_3 system with a CR = 1.6, the structure and the dissolution rate of $Na_2O{\cdot}70Al_2O_3$ remained at intermediate stable values. For $Na_2O{\cdot}xAl_2O_3$ and the first blank Al_2O_3 sample β-Al_2O_3, the peak intensities were 1934, 1452, 1271, and 0 cps respectively. The dissolution rate of aluminum oxide in the electrolyte was 0.72, 0.64, 0.61, and 0.22 g Al_2O_3/100 g melt from 0–5 min. However, due to the lack of the variables of temperature and CaF_2 and LiF additives, the solubility of $Na_2O{\cdot}xAl_2O_3$ in this system cannot be further explored. The solubility of this specimen under these conditions was verified.

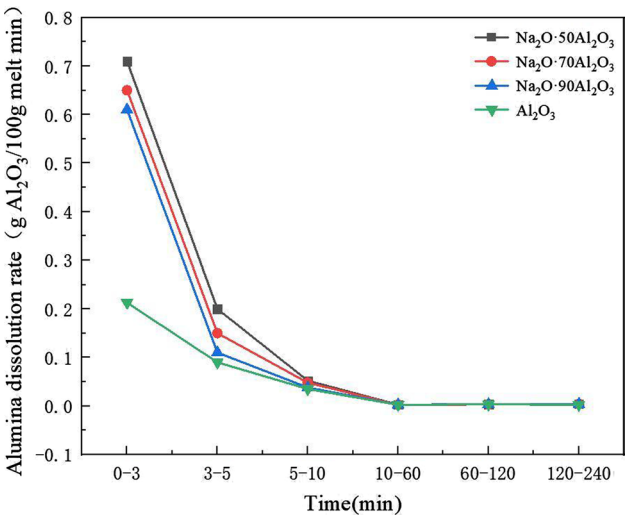

Fig. 4 The dissolution rate of different MR of alumina in electrolyte

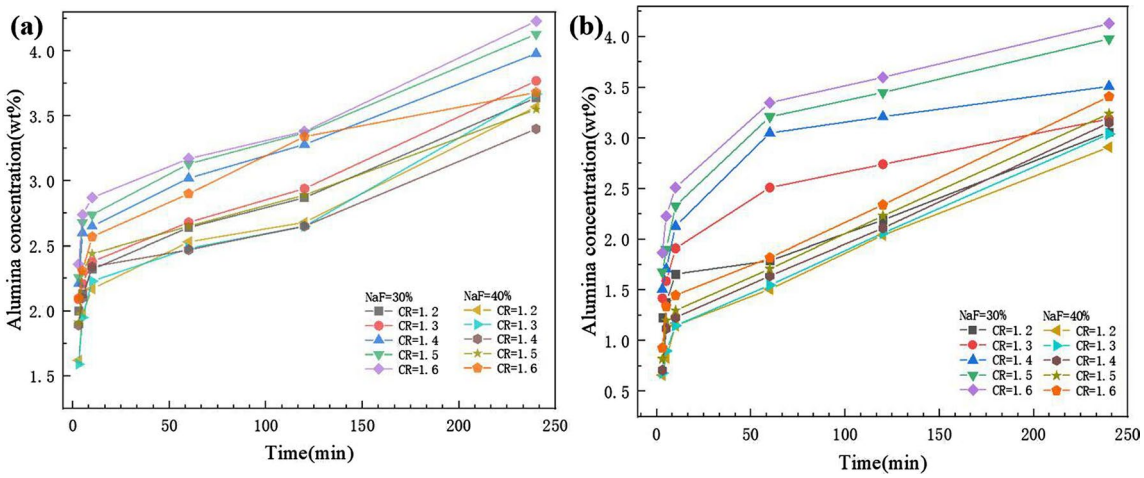

Fig. 5 Effect of CR on the dissolution properties of aluminum oxide. The numbers in the figure indicate that sample **a** was $Na_2O{\cdot}70Al_2O_3$, and sample **b** was blank

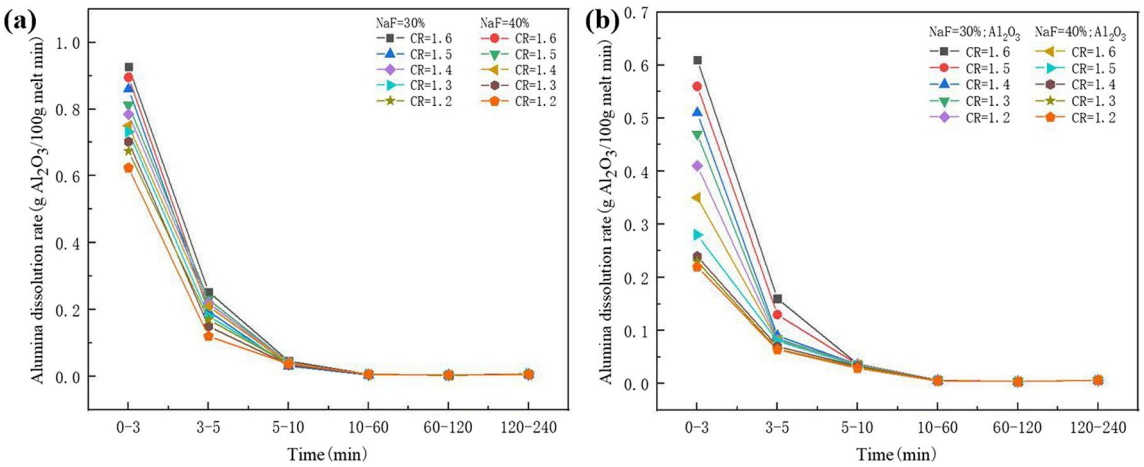

Fig. 6 The dissolution rate of alumina in each time period. The numbers in the figure indicate that sample **a** was $Na_2O{\cdot}70Al_2O_3$, and sample **b** was blank

Experiments were performed to determine the solubility of the $Na_2O{\cdot}70Al_2O_3$ sample's temperature at 850 °C in NaF-KF-AlF_3 electrolytes with CR = 1.2, 1.3, 1.4, 1.5, and 1.6. The variables were the CR and sodium fluoride amounts of 30 and 40 mol%. The experimental results are shown in Fig. 5.

The alumina solubility of $Na_2O{\cdot}70Al_2O_3$ and Al_2O_3 in the electrolyte was greatly improved as the reaction time increased. Compared with the blank Al_2O_3 sample, the dissolution performance of $Na_2O{\cdot}70Al_2O_3$ in the electrolyte was better than that of the blank Al_2O_3 sample from 0–10 min. The concentration difference between $Na_2O{\cdot}70Al_2O_3$ and the blank Al_2O_3 sample gradually decreased and eventually stabilized from 60–240 min. As the CR of the electrolyte increased, so did the KF content in the electrolyte, while the AlF_3 content decreased. Increasing the KF content increased the saturation solubility point from 5.65 to 7.46 wt%, which reduced the mass-transfer limitations of alumina in the electrolyte and accelerated the dissolution rate of $Na_2O{\cdot}70Al_2O_3$ in the molten salt. This has also been proven by other researchers [20–22].

For each time period, the experimental conditions were set as CR = 1.2–1.6 and NaF = 30 and 40 mol% (Fig. 6).

As the dissolution time progressed, the dissolution rate of alumina decreased gradually. Form 0–3 min (CR = 1.6, and NaF = 30 and 40 mol%), the dissolution rate of alumina was higher than that of other CR. Figure 6 shows that changing the CR also affected the dissolution rate of alumina in the electrolyte between $Na_2O{\cdot}70Al_2O_3$ and the blank Al_2O_3 sample. The effect on the blank Al_2O_3 sample was stronger. At the same NaF content, increasing the CR increased the dissolution rate of $Na_2O{\cdot}70Al_2O_3$ and the blank Al_2O_3 sample in the electrolyte by about 1.5 times.

The dissolution rate of alumina in the electrolyte changed obviously at 0–3 min for NaF = 30 mol% and 40 mol%. The dissolution rates of $Na_2O{\cdot}70Al_2O_3$ and the blank Al_2O_3 sample increased by 0.25 and 0.16 (g Al_2O_3/100 g melt), respectively, when CR = 1.2–1.6. According to the above analysis, when the NaF content was constant and the CR increased, the solubility of the blank Al_2O_3 sample and the dissolution rate of alumina were lower than those of $Na_2O{\cdot}70Al_2O_3$.

Compared with $Na_2O{\cdot}70Al_2O_3$, the different dissolution performances and rates of the blank Al_2O_3 sample increased with the NaF content. When the CR was constant, the dissolution rate of alumina and its concentration in the electrolyte with 30 mol% NaF were higher than that of alumina in the electrolyte with 40 mol% NaF.

According to the experimental results, increasing the NaF content slowed the dissolution rate of alumina in the electrolyte. According to the dissolution rate of alumina, upon gradually increasing the NaF content and CR, the influence of CR had a greater effect than the NaF content.

3.4 Study on dissolution kinetics of Al_2O_3

Study on the influence of dissolution rate of alumina with time. T = 850 ℃, CR = 1.2 and 1.6, and NaF = 30 mol%. The results are shown in Fig. 7.

Figure 7 shows that the concentration of aluminum oxide in the molten salt increased with time. In the first 5 min, upon increasing the experimental time, the solubility of aluminum oxide in the electrolyte showed a linear increase. However, after 5 min, this increase gradually slowed.

It can be seen in ref. [19] that the dissolution rate of aluminum oxide in the electrolyte increased linearly with the reaction time. The part in which the dissolution rate of aluminum oxide in the electrolyte increased in a curve with the reaction time and followed the zero-order law. The part of the curve in which the dissolution rate of aluminum oxide in the electrolyte increased followed the first-order law. The reaction rate constants of these two laws reflect the dissolution rate of alumina in the electrolyte.

A zero-order reaction refers to a chemical reaction whose reaction rate is proportional to the zeroth power of reactant concentration. The reaction rate equation is expressed as:

$$C_a - C_0 = -kt_a \tag{6}$$

where t_a is the time, C_a is the dissolution rate of alumina at the time t_a, C_0 is the initial dissolution rate, and k is the reaction rate constant.

It can be seen from the formula of the zero-order reaction rate that the concentration of $Na_2O{\cdot}70Al_2O_3$ in the electrolyte increased with the reaction in the first 5 min of the experiment. When the reaction continued, the concentration of reactants in the molten salt decreased gradually. Based on these conditions, the alumina dissolution rate at 10 min can be used as the initial dissolution rate. The sampling time of the linear portion was 0, 1, 3, and 5 min respectively, as shown in Supplementary Table S-I.

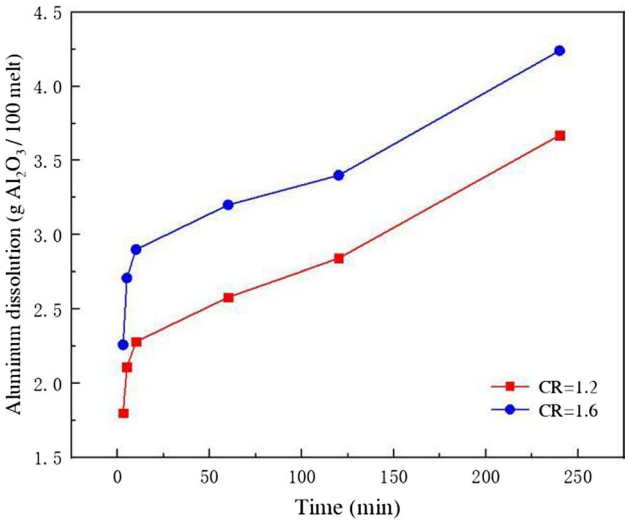

Fig. 7 Relationship between solubility of $Na_2O{\cdot}70Al_2O_3$ and dissolution time in molten salt

The alumina dissolution rate at 5 min was used as the initial dissolution rate. To facilitate the formula calculation, the time was arranged in reverse order. That is, the fifth minute of the original experiment is time zero, the third minute of the original experiment is the first minute, the first minute of the original experiment is the third minute, and the zero time of the original experiment is the fifth minute. The results of data conversion are shown in Supplementary Table S-II.

To linearly fit the relationship between alumina dissolution rate and time with CR = 1.2 and 1.6, Supplementary Table S-II and Table S-II were combined, and the results are shown in Supplementary Fig. S-2.

After fitting, the zero-order reaction rate expression of CR = 1.2 and 1.6 can be obtained:

$$C_a - C_0 = -0.13t_a - 0.0121 \quad R^2 = 0.9865 \tag{7}$$

$$C_a - C_0 = -0.47t_a - 0.0561 \quad R^2 = 0.9781 \tag{8}$$

The zero-order reaction rate equation had a good fit when *CR* = 1.2 and 1.6. Through calculation, when the CR = 1.2 and 1.6, the *k* values in the zero-order reaction rate equation were 0.13 and 0.47 ((g Al_2O_3/100 g melt)·min^{-1}·L^{-1}), respectively.

The first-order reaction rate equation is:

$$1n\left(C_a\right) - 1n\left(C_0\right) = -kt_a \tag{9}$$

It can be seen from the first-order reaction rate formula that the concentration of Al_2O_3 in the electrolyte decreased gradually as the reaction proceeded after 5 min of the experiment. Based on this, the alumina dissolution rate after 120 min was used as the initial dissolution rate. The sampling time of the linear portion was 30, 60, 90, and 120 min respectively, as shown in Supplementary Table S-III.

Similarly, at 120 min, the dissolution rate of alumina was taken as the initial dissolution rate. The logarithm of the data in supplementary Table S-III was taken to obtain supplementary Table S-IV.

To linearly fit the relationship between alumina dissolution rate and time with CR = 1.2 and 1.6, Supplementary Table S-III and Table S-IV were combined, and the results are shown in Supplementary Fig. S-3.

The first-order reaction rate expression with CR = 1.2 and 1.6 was obtained after fitting.

$$\ln\left(C_a/C_0\right) = -0.0108t_a + 0.0332 \quad R^2 = 0.9665 \tag{10}$$

$$\ln\left(C_a/C_0\right) = -0.0122t_a + 0.0371 \quad R^2 = 0.9977 \tag{11}$$

The fitting degree of the first-order reaction rate equations when CR = 1.2 and 1.6 was better. The *k* values in the first-order reaction rate equation were 0.0108 and 0.0122 ((g Al_2O_3 /100 g melt)·min^{-1}·L^{-1}), respectively.

The zero-order reaction rate constant of CR = 1.2 and 1.6 was larger, which also indicates that the dissolution rate of aluminum oxide in the electrolyte with CR = 1.2 and 1.6 was faster in the first 5 min after the experiment. However, from their first-order reaction rate constants upon increasing the time, the difference between the first-order reaction rate constants for CR = 1.2 and 1.6 gradually decreased, and the dissolution rate of aluminum oxide in the electrolyte gradually became the same.

The dissolution of aluminum oxide in the electrolyte can be explained by oxyfluoride, which was produced by the exchange of oxygen ions and fluoride ions. In the experiment, the KF content of the electrolyte was more than 10 wt%. In the NaF-KF-AlF_3 system, the content of AlF_5^{2-} was high, which promoted the formation of $Al_2OF_6^{2-}$ [14]. At the beginning of the experiment, the content of aluminum oxide in the electrolyte was low. Because the concentration of aluminum oxide in the electrolyte increased rapidly, aluminum ions and oxygen ions complexed and combined into the melt structure. Because the oxygen content in the melt was low, the electrolyte easily absorbed aluminum oxide, and the dissolution of aluminum oxide followed the zero-order law.

Upon gradually increasing the alumina concentration, the AlF_5^{2-} content decreased, and AlF_6^{3-} became the dominant species. The coordination number increased from 5 to 6, that is, the Al-O-F complex ion changed from $Al_2OF_6^{2-}$ to $Al_2O_2F_4^{2-}$, making it difficult to absorb oxygen and reducing the dissolution rate of alumina in the electrolyte [23]. Therefore, the dissolution of alumina in electrolyte followed the first-order reaction law.

To sum up, the dissolution rate of alumina in electrolyte depended on the rate constant of the zero-order reaction, that is, the sum of the dissolved amount of alumina in the first 5 min.

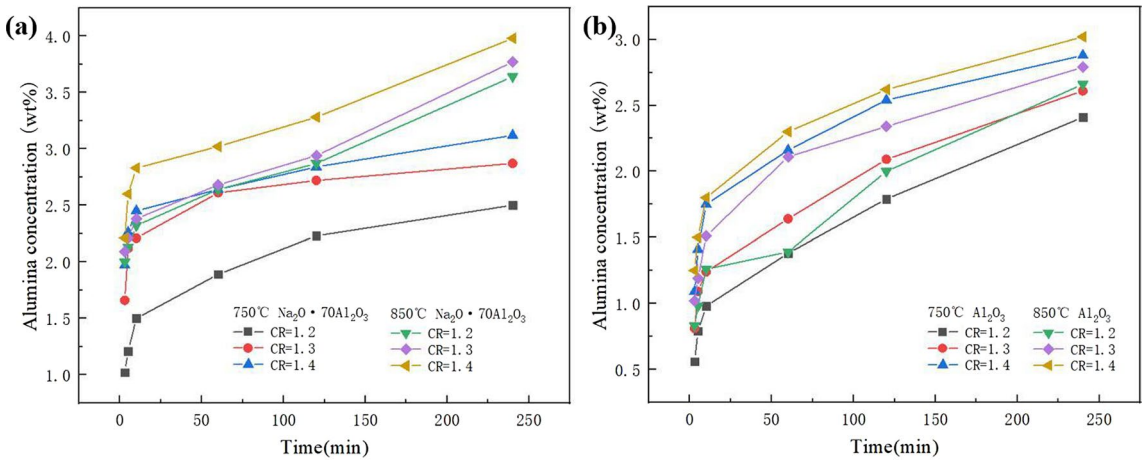

Fig. 8 Effect of different temperatures on the dissolution properties of $Na_2O{\cdot}70Al_2O_3$. The numbers in the figure indicate that sample **a** is $Na_2O{\cdot}70Al_2O_3$, and sample **b** was blank

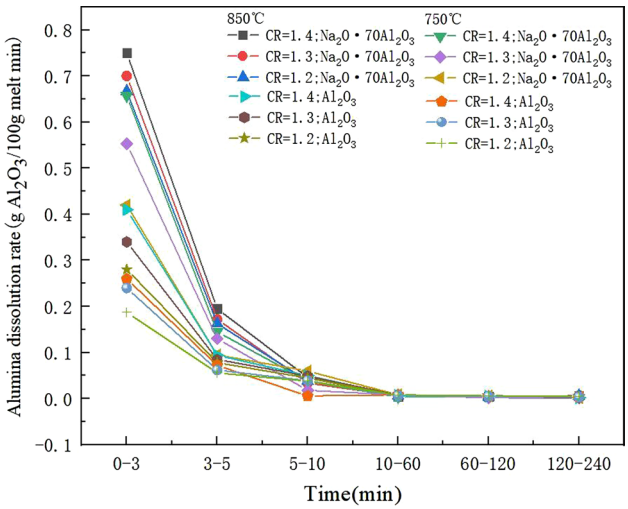

Fig. 9 The dissolution rate of alumina at different temperatures

3.5 Effect of temperature on the solubility of $Na_2O{\cdot}70Al_2O_3$ in electrolytes

The effect of temperature on the solubility of alumina was also investigated in the NaF-KF-AlF_3 system at CR is 1.2, 1.3, and 1.4, and NaF = 30 mol%. The results are shown in Fig. 8.

The concentration of alumina in the electrolyte increased significantly when the temperature increased from 750 to 850 °C. After 120 min, the concentration of alumina in the electrolyte increased slowly and gradually became saturated.

Two groups of samples at different temperatures were compared with the blank Al_2O_3 sample. Upon increasing the CR, the concentration difference between $Na_2O{\cdot}70Al_2O_3$ and the blank Al_2O_3 sample gradually increased, and the concentration difference between $Na_2O{\cdot}70Al_2O_3$ and the blank Al_2O_3 sample was the greatest when the temperature was 850 ℃ and the reaction time was 3 min. When the reaction tended towards saturation (240 min), there was almost no concentration difference. The experimental results show that the lower temperature, the lower the oxygen content of $Na_2O{\cdot}70Al_2O_3$ in NaF-KF-AlF_3, and decreasing the oxygen content decreased the alumina concentration.

The dissolution rate of $Na_2O{\cdot}70Al_2O_3$ in the NaF-KF-AlF_3 system was investigated under the same CR and sodium fluoride amount with the temperature as the variable. The experimental conditions were: CR = 1.2–1.4, NaF content of 30 mol%, and temperature of 750 °C and 850 °C. The experimental results are shown in Fig. 9.

At the same temperature, the dissolution rate of alumina in the two groups increased upon increasing the CR between 0 and 3 min. At 750 ℃, the dissolution rate of $Na_2O{\cdot}70Al_2O_3$ in NaF-KF-AlF_3 increased by 0.85 (g Al_2O_3/100 g

melt) with a CR of 0.1. The dissolution rate of $Na_2O{\cdot}70Al_2O_3$ in the blank Al_2O_3 sample increased by 2.83–1.83 times compared with $Na_2O{\cdot}70Al_2O_3$. At 850 ℃, the dissolution rate of $Na_2O{\cdot}70Al_2O_3$ in the electrolyte increased by 1.11 (g Al_2O_3/100 g melt). Compared with $Na_2O{\cdot}70Al_2O_3$, the dissolution rate of the blank Al_2O_3 sample increased by 2.2–2.5 times. In general, a higher temperature had a greater influence on the dissolution rate of the sample. Upon increasing the CR, the difference between the dissolution rate of alumina increases gradually at both temperatures. From 0–10 min, the dissolution rates of $Na_2O{\cdot}70Al_2O_3$ and Al_2O_3 in the electrolyte at 850 ℃ were 1.3–1.4 times higher than those at 750 ℃.

3.6 Effect of CaF_2 and LiF on the solubility of $Na_2O{\cdot}70Al_2O_3$ in electrolytes

Since it has been determined in the exploratory experiments that the experimental time had a clear trend at 60 min, the time was set to 60 min in subsequent experiments to study the concentration of $Na_2O{\cdot}70Al_2O_3$ in NaF-KF-AlF_3-CaF_2-LiF electrolyte. This was done to reduce the errors caused by gradual saturation over time. The effect of the CR and CaF_2 and LiF contents on the solubility of alumina in the electrolyte melt was investigated in the NaF-KF-AlF_3-CaF_2-LiF electrolyte system under the same experimental conditions (CR is 1.3 and 1.4, NaF addition of 30%, and temperature of 750 °C). The obtained data are shown in Fig. 10.

As shown in Fig. 10, the concentration of alumina was negatively correlated with the CaF_2 and LiF content. As the calcium fluoride content increased, the CR decreased, resulting in a decrease in the concentration of alumina in the melt. When the LiF content increased from 0 to 2.5 wt%, for every 1 wt% increase in LiF content, the concentration of alumina decreased by about 0.12 wt%, respectively. It is evident that when the CR was decreased, the effect of LiF and CaF_2 on the alumina dissolution rate also decreased.

In an alumina solubility experiment, Yan et al. [16] reported that for every 1 wt% LiF that was added to a K_3AlF_6 melt with an AlF_3 content of 33 wt% at 700 ℃, the solubility of alumina decreased by 0.37 wt%. In recent years, many scholars have studied the solubility of lithium salts in alumina in traditional aluminum electrolysis systems. [24, 25] The results have shown that in electrolyte melts, Li^+ has a small ionic radius and is more attractive to anions such as AlF_4^- and AlF_5^{2-}. Moreover, upon increasing the LiF content, the content of free fluoride ion F^- in molten salt increased slightly. Therefore, when Li^+ is added to the melt, the Al_2O_3 reaction is inhibited, and the solubility of molten Al_2O_3 in the electrolyte is reduced. When CaF_2 is added to the melt, the contents of AlF_4^- and AlF_5^{2-} will also be reduced, and the solubility of alumina in the bath will be eventually reduced. In an electrolyte with the same amount of CaF_2 and LiF, upon increasing the CR, the concentration of alumina in the $Na_2O{\cdot}70Al_2O_3$ and blank Al_2O_3 sample electrolyte also increased, then the concentration of $Na_2O{\cdot}70Al_2O_3$ in the electrolyte underwent a smaller change than that of the blank Al_2O_3 sample. When the amount of additives was the same, the greater the CR, the better the concentration of $Na_2O{\cdot}70Al_2O_3$ and the blank Al_2O_3 sample in the electrolyte. Under the same CR, the influence of CaF_2 on the concentration of alumina in the electrolyte is less than that of LiF at the same weight percentage.

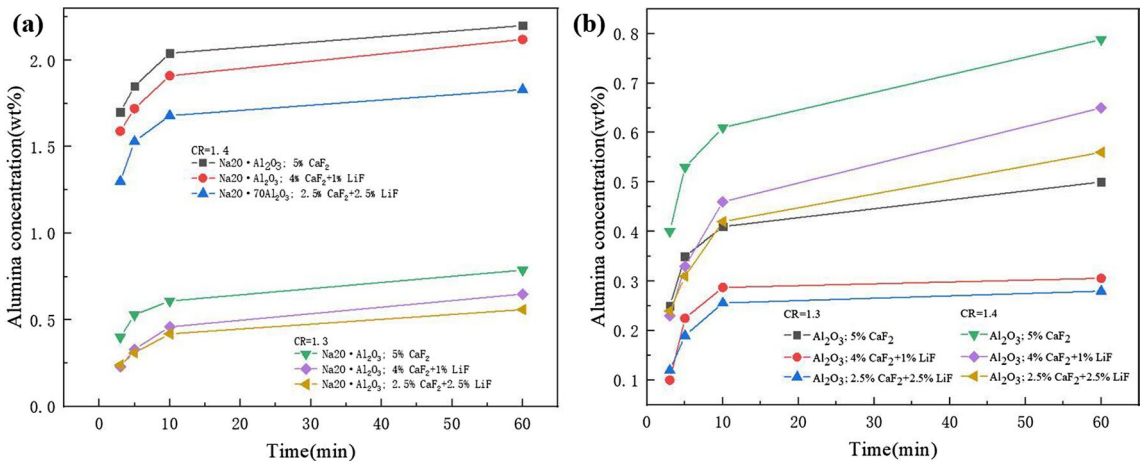

Fig. 10 Effect of CaF_2 and LiF on the solubility of $Na_2O{\cdot}70Al_2O_3$ in NaF-KF-AlF_3 electrolyte. The numbers in the figure indicate that sample **a** is $Na_2O{\cdot}70Al_2O_3$, and sample **b** was blank

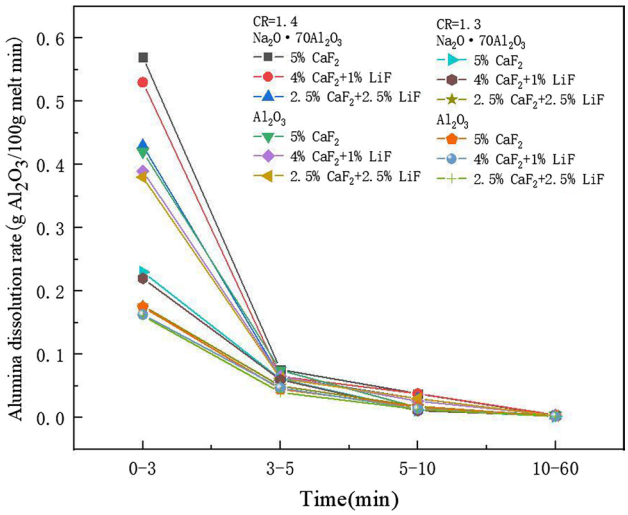

Fig. 11 The dissolution rate of alumina in electrolytes containing CaF_2 and LiF

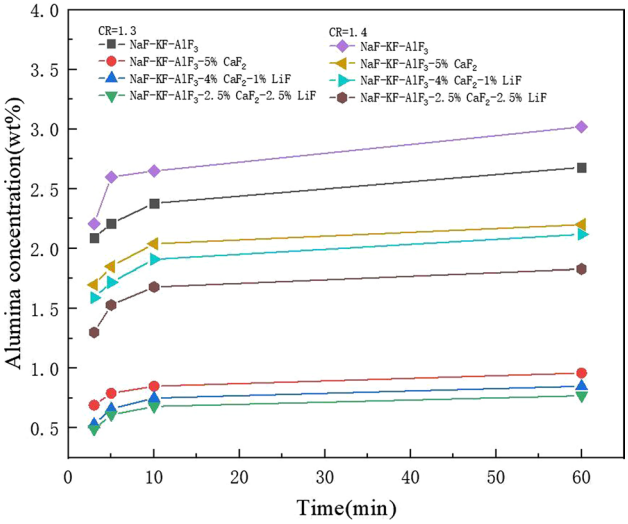

Fig. 12 Effect of NaF-KF-AlF_3 and NaF-KF-AlF_3-CaF_2-LiF on the dissolution properties of $Na_2O \cdot 70Al_2O_3$.

The dissolution rate of alumina in NaF-KF-AlF_3-CaF_2 (5 wt%, 4 wt%, 2.5 wt%)-LiF (0 wt%, 1 wt%, 2.5 wt%) electrolyte systems was investigated using calcium fluoride and lithium fluoride as variables. The experimental conditions were: CR = 1.3–1.4, NaF content of 30 mol%, and temperature of 750 °C. The experimental results are shown in Fig. 11.

While the dissolution rate of alumina in the electrolyte gradually decreased. From 0–3 min, the dissolution rate of alumina in the electrolyte with a CR = 1.4 was faster than that of alumina with a CR = 1.3. When CR = 1.4, the dissolution rate of alumina in the electrolyte with $Na_2O \cdot 70Al_2O_3$ was 1.3 times higher than that of the Al_2O_3 sample. When CR = 1.3, the dissolution rate of $Na_2O \cdot 70Al_2O_3$ in the electrolyte was about twice that of the Al_2O_3 sample. At the same CR, there was a significant difference in the dissolution rate of alumina in NaF-KF-AlF_3-CaF_2, and the difference between the two samples was about 0.1 and 0.05 (g Al_2O_3/100 g melt min), respectively. At 3–5 min, the dissolution rate of alumina in the electrolyte followed the above rule. However, the dissolution rate of alumina in different electrolytes in 5–10 min changed irregularly, and there was little difference. At 10–60 min, the dissolution rate of alumina with different electrolytes was small, so no specific analysis was performed.

Changes in the alumina concentration with the CaF_2 and LiF contents in the NaF-KF-AlF_3 electrolyte are studied for $Na_2O \cdot 70Al_2O_3$ when the CR is 1.3 and 1.4, the NaF content is 30 mol%, and the temperature is 750 °C. The experimental results are shown in Fig. 12.

Adding CaF_2 alone or the addition of CaF_2 and LiF mixture to the NaF-KF-AlF_3 electrolyte system decreased the solubility of $Na_2O \cdot 70Al_2O_3$ in alumina. The concentration of alumina in the NaF-KF-AlF_3 electrolyte system with $Na_2O \cdot 70Al_2O_3$ increased gradually upon increasing the CR of the NaF-KF-AlF_3-CaF_2 (2.5 wt%, 4 wt%, 5 wt%)-LiF (2.5 wt%, 1 wt%, 0 wt%) electrolyte. In comparison, the effect of the alumina concentration in the electrolyte with a CR = 1.3 was much greater

than that at a CR = 1.4. The concentration and the dissolution rate of alumina in the conventional ternary electrolyte system were higher than those in the electrolytes containing CaF_2 and LiF.

4 Conclusions

$Na_2O{\cdot}xAl_2O_3$ samples were formed by adding Na_2O to Al_2O_3. After being calcined at 1000 ℃, the structure changed, and β-Al_2O_3 was produced. However, β-Al_2O_3 promoted the dissolution rate of the sample in the electrolyte, so the dissolution rate of alumina was improved by increasing the Na_2O content in Al_2O_3.

In a NaF-KF-AlF_3-based low-temperature electrolyte system, $Na_2O{\cdot}xAl_2O_3$ showed a faster alumina dissolution rate than Al_2O_3. The higher the Na_2O content in alumina, the faster the dissolution rate. When the NaF content in NaF-KF-AlF_3 was in the range of 30–40 mol%, the alumina dissolution rate of $Na_2O{\cdot}xAl_2O_3$ in the molten salt was 1–2 times higher than that of Al_2O_3. When the temperature was in the range of 750–850 ℃, the alumina dissolution rate of $Na_2O{\cdot}xAl_2O_3$ in the molten salt was 1.5–3 times higher than that of Al_2O_3. The dissolution rate of $Na_2O{\cdot}70Al_2O_3$ and the blank Al_2O_3 sample in the electrolyte increased when the temperature and CR of the molten salt increased. However, the dissolution rate of alumina decreased upon increasing the NaF content.

The reaction rate constant of the zero-order reaction was larger than those of the first-order reaction rate during alumina dissolution. The dissolution rate of alumina in each time period and the rate constants of the two rate laws showed that the dissolution rate of alumina depended on the amount of alumina absorbed by the electrolyte in the first five minutes of the experiment.

At a constant CR and temperature, adding CaF_2 and LiF to the ternary electrolyte reduced the difference between the dissolution rate between the blank Al_2O_3 sample and $Na_2O{\cdot}70Al_2O_3$ in the molten salt by 1.7–3.2 times. The influence of CaF_2 on the dissolution rate of alumina in the electrolyte was weaker than that of LiF.

Acknowledgements The financial support from NSFC 52064030, Yunnan industrial talent project YNQR-CYRC-2018-013, supported by Yunnan Major Scientific and Technological Projects (grant No. 202202AG050007, and 202202AG050011), are acknowledged.

Author contributions YK and HY wrote the main manuscript text, while ZL and YY prepared the drawings and tables. All the authors reviewed the manuscript. All authors read and approved the final manuscript.

Data availability All data generated or analyzed during this study are included in this published article (and its supplementary information files).

Declarations

Competing interests The authors declare no competing interests.

References

1. Zhao CF, Zhang SZ, Huang X. Study on reducing PFCs emissions in aluminum industry[J]. Light Met China. 2008;10:26.
2. Wang B, Liang F, Dai YN. Research status and future development prediction of inert anode for aluminum electrolysis[J]. Light Met China. 2018;12:30.
3. Zaikov Y, Khramov A, Kovrov V, Kryukovsky V, Apisarov A, Tkacheva O, Chemesov O, Shurov N. Electrolysis of aluminum in the low melting electrolytes based on potassium cryolite[J]. Metals Mater Soc. 2008;2008:505.
4. Sleepy WC, Kensington N, Cochran CN. Bench scale electrolysis of alumina in sodium fluoride-aluminium fluoride melts below 900℃[J]. Aluminium. 1979;55:1089. https://doi.org/10.1002/9781118647851.ch159.
5. Welch BJ. Aluminum production paths in the new millennium[J]. JOM. 1999;5:24. https://doi.org/10.1007/s11837-999-0036-4.
6. Padamata SK, Yasinskiy AS, Polyakov PV. Behaviour of aluminium oxide in KF-AlF_3-Al_2O_3 melts and suspensions[J]. New J Chem. 2020;44:5152. https://doi.org/10.1016/j.ceramint.2020.01.180.

7. Huang LQ, Liu ZW, Yan HW. Research Status of low temperature electrolytes system for Aluminum electrolysis [J]. Nonferr Met Eng China. 2020;10:42.
8. Apisarov A, Dedyukhin A, Nikolaeva E. Liquidus temperatures of cryolite melts with low cryolite ratio[J]. Metall Mater Trans B. 2011;42B:236. https://doi.org/10.1007/s11663-010-9462-5.
9. Liao XA, Bao SC, Sun Y. Review of carbon-free aluminum electrolysis technology[J]. Light Met China. 2019;3:1.
10. Beck TR. A new energy-efficient and environmentally friendly process to produce aluminum[J]. JOM. 2013;65:267. https://doi.org/10.1007/s11837-012-0517-8.
11. Wang M, Yan HW. Research Progress of KF-NaF-AlF_3-X low temperature electrolyte system[J]. Light Met China. 2009;9:28.
12. Hives J, Fellner P, Thonstad J. Transport numbers in the molten system NaF-KF-AlF_3-Al_2O_3[J]. Ionics. 2013;19:315. https://doi.org/10.1007/s11581-012-0736-6.
13. Kuang G, Kuang C. Production of anhydrous aluminum fluoride by three-stage combined process[J]. Light Metals China. 2002;03:23. https://doi.org/10.3969/j.issn.1002-1752.2002.03.007.
14. Lv XJ, Han ZX, Zhang HX. Ionic structure and transport properties of KF-NaF-AlF_3 fused salt: a molecular dynamics study[J]. Phys Chem Chem Phys. 2019;21:7474. https://doi.org/10.1039/C9CP00377K.
15. Yan HW, Liu ZW, Ma WH, Huang LQ, Wang CZ, Liu YX. KF-NaF-AlF_3 system: liquidus temperature and phase transition[J]. JOM. 2019;72:247. https://doi.org/10.1007/s11837-019-03909-7.
16. Yan HW, Yang JH, Li WX. Surface tension and density in the KF-NaF-AlF_3-based electrolyte[J]. Chem Eng Data. 2011;11:56. https://doi.org/10.1021/je2005825.
17. Peng JP, Wei Z, Di YZ, Wang YW, Sun T. Towards improved current efficiency of HallHéroult cells by using a novel cathode and process parameters[J]. JOM. 2020;72:239. https://doi.org/10.1007/s11837-018-3245-x.
18. Stebbins JF, Farnan I, Dando N, et al. Solids and liquids in the NaF-AlF_3-Al_2O_3 system: a high-temperature NMR study[J]. Am Ceram Soc. 1992;75:3001. https://doi.org/10.1111/j.1151-2916.1992.tb04378.x.
19. Isaeva LA, Braslavskii AB, Polyakov PV. Effect of the content of the α-phase and granulometric composition on the dissolution rate of alumina in cryolite-alumina melts. Russ J Non-Ferrous Met. 2009;50:600. https://doi.org/10.3103/S1067821209060078.
20. Hu XW, Li L, Li H. Thermal decomposition of ammonium hexafluoro aluminate and preparation of aluminum fluoride[J]. Nonferrous Met China. 2011;21:2087. https://doi.org/10.1016/S1003-6326(11)60977-1.
21. Zhou CH, Ma SL, Li GX, Shen JY. Study on a new low temperature aluminum electrolyte system—solubility and dissolution rate of Alumina[J]. Nonferr Met Eng China. 1998;2:82.
22. Robert E, Olsen JE, Danek V. Structure and thermodynamics of alkali fluoride alumina melts, Vapor Pressure, Solubility, and Raman Spectroscopic Studies[J]. Phys Chem B. 1997;101:9447. https://doi.org/10.1021/jp9634520.
23. Suzdaltsev AV, Nikolaev AY, Zaikov YP. Towards the stability of low-temperature aluminum electrolysis. J Electrochem Soc. 2021;4:168. https://doi.org/10.1149/1945-7111/ABF87F.
24. Li DX, Wei QB, Li Y. Study on aciding lithium fluoride to aluminum electrolyte[J]. Light Met China. 1980;3:16.
25. Cao AL, Guo L, Li JJ. Spatial-temporal distribution of alumina concentration in typical areas of 400 kA aluminum reduction cell [J]. Nonferrous Met China. 2018;6:23.